

Can strong gravitational lensing distinguish naked singularities from black holes?

Satyabrata Sahu*, Mandar Patil†, D. Narasimha‡, Pankaj S. Joshi§
*Tata Institute of Fundamental Research
Homi Bhabha Road, Mumbai 400005, India*

In this paper we study gravitational lensing in the strong field limit from the perspective of cosmic censorship, to investigate whether or not naked singularities, if at all they exist in nature, can be distinguished from black holes. The spacetime which we explore from this perspective is JMN metric which represents a spherically symmetric solution to the Einstein field equations with anisotropic pressure and contains a naked singularity at the center. JMN geometry is matched with the Schwarzschild metric to the exterior at a finite radius. This metric was recently shown to be a possible end state of gravitational collapse of a fluid with zero radial pressure. In the presence of the photon sphere gravitational lensing signature of this spacetime is identical to that of Schwarzschild black hole with infinitely many relativistic images and Einstein rings, all of them located beyond a certain critical angle from optic axis and the inner relativistic images all clumped together. However, in the absence of the photon sphere, which is the case for a wide range of parameter values in this spacetime, we show that we get finitely many relativistic images and Einstein rings spaced reasonably apart from one another, some of which can be formed inside the critical angle for the corresponding Schwarzschild black hole. This study suggests that the observation of relativistic images and rings might, in principle, allow us to unravel the existence of the naked singularity in the absence of the photon sphere. Also the results obtained here are in contrast with the earlier investigation on JNW naked singularities where it was shown that the radial caustic is always present in the absence the photon sphere, which is not the case with JMN geometry where radial caustic is absent. We also point out the practical difficulties that might be encountered in the observation of the relativistic images and suggest that new dedicated experiments and techniques have been developed in future for this purpose.

PACS numbers: 95.30.Sf, 04.20.Dw, 04.70.Bw, 98.62.Sb

I. INTRODUCTION

Deflection of light by massive bodies and therefore the phenomenon of gravitational lensing is a prediction of General Relativity which has helped in observationally testing Einstein theory against Newtonian gravity. In fact it was one of the first successfully verified predictions of General Relativity in 1919. Since then there has been numerous studies of gravitational lensing, both theoretically and observationally. But for good reasons, mostly these have been confined to the weak field approximation. The last decade, however, has seen a great rise in the interest in gravitational lensing in the strong field regime. This is important as a test of General Relativity in itself (because almost all generalizations of General Relativity should by construction reproduce the same weak field limit), as well as for the testing of various compact object scenarios in General Relativity (because they too have the same weak field). In particular, it is important to study whether and how strong field lensing can distinguish between various end states of gravitational collapse of massive matter clouds (such as a massive star continually collapsing at the end of its life cycle), viz. black

hole and naked singularity. This is also important from the perspective of the cosmic censorship conjecture.

Cosmic censorship conjecture was proposed by Penrose in order to get rid of the naked singularities in the real world around us [1]. However the cosmic censorship conjecture is not yet proved even several decades after it was put forward. There were many studies recently where it was shown that the black holes as well as naked singularities are formed in a continual gravitational collapse of a matter cloud of reasonable matter field starting from a regular initial data [2, 3]. Thus naked singularities might occur in nature. Their occurrence or otherwise is hard to infer from purely theoretical investigations as it is extremely difficult to solve the Einstein equations in an astrophysically realistic scenario. Thus one could take a phenomenological approach, where the consequences of the occurrence of the naked singularities computed theoretically are compared with the observations to either confirm or rule out the existence of the naked singularities. In this paper we explore the gravitational lensing from such a perspective. We note here that the strong gravitational lensing in JNW spacetime [4, 5], lensing in post-Newtonian framework for Kerr geometry [6] as well as for the rotating generalization of JNW spacetime [7] and the investigation of the shape and the position of the shadow in Kerr and Tamimatsu-Sato spacetimes [8–10] has been done recently to address the same question.

Early works on strong field lensing were by Darwin [11, 12], who studied the behavior of null geodesics in strong field regime of Schwarzschild black hole and

*Electronic address: satyabrata@tifr.res.in

†Electronic address: mandarp@tifr.res.in

‡Electronic address: dna@tifr.res.in

§Electronic address: psj@tifr.res.in

pointed out the divergence of Einstein deflection angle as the distance of closest approach of the geodesics approaches photon sphere. Strong field lensing with a lens equation was studied by Virbhadra and Ellis [13], who examined strong field lensing in Schwarzschild black holes and showed that there could in principle be infinite relativistic images on each side of the black hole when a light ray with small enough impact parameter (distance of closest approach close enough to photon sphere) goes around one or several times around the black hole before reaching the observer. Earlier, lens equation for spherically symmetric static spacetimes that goes beyond the weak field small-angle approximation was studied by Virbhadra, Narasimha and Chitre in [4]. The Virbhadra-Ellis type lens equation has also been applied to boson star by Dąbrowski and Schunck [14], to a fermion star by Bilić, Nikolić and Viollier [15]. As one of the first steps towards using strong field lensing to probe the cosmic censorship question, Virbhadra and Ellis have used this lens equation to study and compare gravitational lensing by normal black holes and by naked singularities modeled by the Janis, Newman, Winicour metric (JNW solution)[5].

It is worthwhile to extend this line of work to other novel, more interesting and if possible more realistic naked singularity models. With this in mind we consider here the class of solutions recently obtained by Joshi, Malafarina and Narayan [16] as end state of certain dynamical collapse scenarios in a toy example. JMN metric is a solution of Einstein field equations with an anisotropic pressure fluid and has a naked singularity at the center. It is matched to the Schwarzschild metric at a certain radius. We refer to it here as JMN naked singularity from now on. It is worthwhile to mention that, not only the presence of the central naked singularity but also the value of the radius at which the interior solution is matched to exterior Schwarzschild geometry plays a crucial role in determining gravitational lensing observables.

We should also mention that exact lens equations were proposed by [17] for arbitrary spacetime and also by [18] for spherically symmetric case. Bozza et al. have defined and analytically calculated strong field limit observables in spherically symmetric spacetimes endowed with a photon sphere [19, 20]. In such a situation strong lensing from various alternatives/modifications of Schwarzschild geometry in modeling the galactic center has been studied. For example lensing from regular black holes was studied in [21] and lensing from stringy black holes was studied in [22]. However the basic qualitative features in a lensing scenario in the presence of a photon sphere is very similar to Schwarzschild case and is ineffective in probing the geometry beyond the photon sphere. Strong field lensing would be much easily able to probe differences from Schwarzschild spacetime if geometry being studied will be without a photon sphere. As we will see for the family of solutions studied in this paper, when the geometry has a photon sphere the lensing signatures are

exactly identical to Schwarzschild black hole case while in the absence of photon sphere it is greatly different. In this work, the galactic supermassive compact object is analyzed as a strong gravity lens to illustrate these characteristics.

This paper is organized as follows. In section II we introduce the basic formalism in brief. In section III we discuss the lens model with galactic supermassive dark object as the lens and in section IV we discuss the lensing signatures when it is modeled as a Schwarzschild black hole. We discuss the naked singularity spacetime we intend to study and lensing in this background in V and compare this with Schwarzschild black hole and JNW solution in VI & VII respectively. In section VIII, we discuss the implications of going beyond point source approximation for our study and in IX we briefly discuss how binary systems could be useful for probing question of cosmic censorship via gravitational lensing. Finally, we discuss the main results and conclude with a general discussion in section X.

II. BASIC FORMALISM

In this section we review the standard gravitational lensing formalism [4, 13] used in this paper to compute the location and properties of the images.

We assume that the spacetime under consideration that is to be thought of as a gravitational lens is spherically symmetric, static and asymptotically flat. We assume that the source and the observer are located sufficiently far away from the lens so that they can be taken to be at infinity for all practical purposes. We also assume that the source is a point-like object, although towards the end of the paper we describe how the results based on the point source assumption would change if the source has a finite extent instead of it being point-like. We assume that the geometrical optics approximation holds good. However we note that if we go arbitrarily close to the singularity, the Riemann curvature might become comparable to the wavelength of the light leading to the breakdown of the geometrical optics approximation.

The gravitational lensing calculations has two important parts. First one is the lens equation which relates the location of the source to the location of the image given the amount of deflection suffered by the light from source to the observer as it passes by the the gravitational lens. The second important component is the deflection of the light encoded in the Einstein deflection angle $\hat{\alpha}(\theta)$ which we define later. We note that the deflection angle is the only input from the General theory of Relativity, and it can be computed by integrating the null geodesics.

A. Lens equation

The lens equation essentially relates the position of the source to that of image. Fig1 is the lens diagram. It is

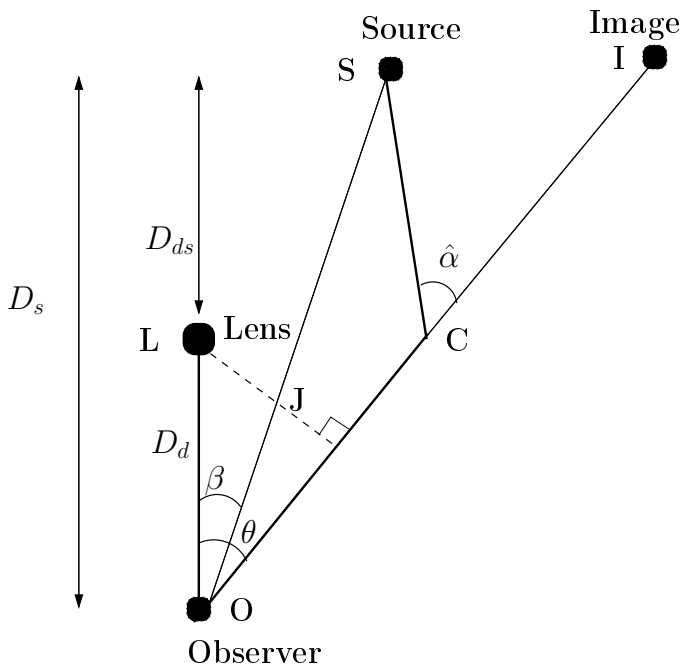


FIG. 1: The lens diagram: Positions of the source, lens, observer and the image are given by S , L , O and I . The distances between lens-source, lens-observer and source-observer are given by D_{ds} , D_d and D_s . The angular location of the source and the image with respect to optic axis are given by β and θ . The impact parameter is given by J .

same as lens diagram given in [13]. The spherically symmetric spacetime under consideration is to be thought of as a lens denoted by L in the lens diagram. The source S and observer O are located faraway as compared to the Schwarzschild radius, from the center of the spacetime in the asymptotic flat region. The line joining lens and the observer is known as the optic axis of the lensing geometry. In the absence of the lens light would have traveled along the line SO and would have made an angle β with respect to the optic axis. Thus β is the source location. In the presence of the lens light gets bent. Let SC and OC be the tangents drawn to the trajectories of the light at the source and the observer. The angle OC makes with the optic axis namely θ depicts the location of the image I . The angle SCI is the Einstein deflection angle $\hat{\alpha}$ which we calculate later in this section. The distances from source to lens, observer to lens and source to observer are given by D_{ds} , D_d and D_s respectively.

The light mostly travels on the lines SC and CO except for the region close to lens where curvature is large and it suffers from a deflection. When the deflection is large, light can go around the lens multiple times.

Here we assume that β is very small i.e. the observer, lens and the source are aligned to a very good approximation. Let LN be the perpendicular drawn to OI from the lens. J here is the impact parameter. From the lens

diagram we get

$$\sin \theta = \frac{J}{D_d}. \quad (1)$$

The location of the source β and the image θ can be related to each other by the following relation from the lens diagram.

$$\tan \beta = \tan \theta - \alpha, \quad (2)$$

where

$$\alpha \equiv \frac{D_{ds}}{D_s} [\tan \theta + \tan (\hat{\alpha} - \theta)]. \quad (3)$$

From the diagram above it is clear that what enters into the lens equation is the deflection angle $\hat{\alpha}$ modulo 2π .

We note that the many versions of the lens equation have been used in the literature depending on the need and convenience. The lens equation 2 used in this paper was derived by Virbhadra and Ellis [13]. It allows for an arbitrarily large deflection of the light. We note that one of the coauthors of this paper (DN) along with Virbhadra and Chitre [4] had worked on a different lens equation in a first investigation of the strong lensing phenomenon with large deflection; but none of the features we describe here change if we use that equation.

B. Deflection angle

One requires the knowledge of the metric of the spacetime to derive the expression for the Einstein deflection angle. Consider general spherically symmetric static spacetime. The metric in the Schwarzschild-like coordinates (t, r, ν, ϕ) can be written as

$$ds^2 = -g(r)dt^2 + \frac{1}{f(r)}dr^2 + r^2d\Omega^2, \quad (4)$$

where $g(r)$ and $f(r)$ are arbitrary functions. Asymptotic flatness demands that $g(r \rightarrow \infty) = f(r \rightarrow \infty) = 1$.

In a gravitational lensing scenario under consideration, source, observer and the lens define a plane. In a spherically symmetric spacetime, the trajectory of the photon is confined to a plane passing through the center which by the appropriate gauge choice can be taken to be the equatorial plane ($\vartheta = \pi/2$). Thus only those light rays emitted by the source, which travel in this plane can possibly reach the observer, ultimately leading to the formation of images and Einstein rings, and this plane can be taken to be the equatorial plane without loss of generality.

The equation of motion for the light ray can be written as

$$U^t = \frac{1}{Jg(r)}, \quad U^\nu = 0, \quad U^\phi = \frac{1}{r^2} \quad (5)$$

and the radial motion is described by the equation

$$\frac{g(r)}{f(r)} \left(\frac{dr}{d\lambda} \right)^2 + V_{eff}(r) = \frac{1}{J^2} \quad (6)$$

where

$$V_{eff} = \frac{g(r)}{r^2} \quad (7)$$

can be thought of as an effective potential for the radial motion. Here $U = (U^t, U^r, U^\theta, U^\phi)$ stands for the velocity of the photon, λ is the affine parameter and as stated earlier, J is the impact parameter.

We can relate the impact parameter J and the distance of closest approach r_0 using (5),(6) and by setting $\frac{dr}{d\phi} = 0$ in the following way

$$J(r_0) = r_0 \sqrt{\frac{1}{g(r_0)}}. \quad (8)$$

The total deflection suffered by the light ray as it travels from the source to the observer (i.e. the deflection angle) as a function of a distance of the closest approach of the light ray to the lens, is $\hat{\alpha}(r_0) = 2 \int_{r_0}^{\infty} \frac{U^r}{U^\phi} d\phi - \pi$ So it is given by

$$\hat{\alpha}(r_0) = 2 \int_{r_0}^{\infty} \left(\frac{1}{f(r)} \right)^{1/2} \left[\left(\frac{r}{r_0} \right)^2 \frac{g(r_0)}{g(r)} - 1 \right]^{-1/2} \frac{dr}{r} - \pi, \quad (9)$$

One important question for lensing in strong field regime is the presence/absence of photon sphere which is a $r = const$ null geodesics. As the distance of closest approach asymptotically approaches the photon sphere, the photon revolves around the lens more and more number of times and the bending angle $\hat{\alpha}$ diverges as the distance of closest approach tends to photon sphere r_{ph} . The maxima/minima of V_{eff} give unstable/stable photon spheres. Thus equation for photon sphere is given by

$$\frac{dg(r)}{dr} = \frac{2g(r)}{r} \quad (10)$$

The effective potential for photons in this geometry gives an idea of the radial behavior of photon trajectories, in particular the turning points for photons. Hence it gives an idea as to when photons coming from infinity get captured and when they can escape back to asymptotia. If $J > J(r_{ph})$ then the photon turns back from radius $r > r_{ph}$ before it reaches the photon sphere. On the other hand if $J < J(r_{ph})$, the photon enters the photon sphere. Whether or not photon is captured or it again comes out after it has entered the photon sphere depends on the behavior of the effective potential in the interior of the photon sphere. Typically in most of the situations photon never comes out once it enters the photon sphere.

C. Lensing observables

We now describe the important lensing observables. For a fixed position of the source, we compute the position of images and their magnifications.

All those values of θ that satisfy the lens equation (2) for fixed values of the source position β yield us the location of the images. In order to do that we must write down the deflection angle as a function of the source position $\hat{\alpha}(\theta)$. This can be achieved using (1),(8).

The cross-section of the bundle of rays gets modified due to the lensing. Liouville's theorem implies that the surface brightness is preserved. Thus the magnification i.e. ratio of the flux of the image to the flux of the source is the ratio of the solid angle subtended by the image to that of the source at the location of the observer.

The total magnification is defined as

$$\mu \equiv \left(\frac{\sin \beta}{\sin \theta} \frac{d\beta}{d\theta} \right)^{-1}. \quad (11)$$

which can be broken down into the tangential and radial magnification in the following way.

$$\mu_t \equiv \left(\frac{\sin \beta}{\sin \theta} \right)^{-1}, \quad \mu_r \equiv \left(\frac{d\beta}{d\theta} \right)^{-1} \quad (12)$$

The sign of the magnification of an image gives the parity of the image. The singularities of the tangential and radial magnification yield the tangential critical curves (TCCs) and radial critical curves (RCCs), respectively in the lens plane and tangential caustic (TC) and radial caustics (RCs) respectively in the source plane.

It is obvious from the expression for the tangential magnification that $\beta = 0$ gives the TC and the corresponding values of θ are the TCCs, also known as Einstein rings (ER). Thus Einstein rings can be obtained by solving for lens equation for $\beta = 0$ i.e, in aligned configuration of source, lens and observer.

Using the lens equation (2) the radial magnification (12) can be written in the following way:

$$\frac{d\beta}{d\theta} = \left(1 - \frac{D_{ds}}{D_s} \right) \frac{\sec^2 \theta}{\sec^2 \beta} - \frac{D_{ds}}{D_s} \frac{\sec^2(\hat{\alpha} - \theta)}{\sec^2 \beta} \left(\frac{d\hat{\alpha}}{d\theta} - 1 \right) \quad (13)$$

It is clear from the expression above that if $\frac{d\hat{\alpha}}{d\theta} < 0$ i.e. when $\hat{\alpha}$ is a monotonically decreasing function, we have $\frac{d\beta}{d\theta} > 0$ and the radial magnification will never diverge. Thus the radial critical curves would be absent, which will be the case for Schwarzschild as well as JMN naked singularity geometry dealt in this paper later .

III. GALACTIC CENTRAL SUPERMASSIVE OBJECT AS A LENS

In this section we describe the gravitational lensing scenario that we would like to focus on in this paper.

The central supermassive dark object in our galaxy is modeled initially as Schwarzschild black hole and in the later section as a naked singularity. The mass of this object is taken to be $M = 2.8 \times 10^6 M_\odot$ which is the mass of the supermassive black hole in our galaxy. Distance of the source from the center of the galaxy is taken to be the distance of the sun from the galactic center $D_d = 8.5 kpc$. Thus, in our example, in the near-aligned configuration the lens is situated midway between the source and the observer i.e. $D_{ds}/D_s = 1/2$. Ratio of mass of the lens to the distance to the observer which would later appear in the calculations is $M/D_d \approx 1.57 \times 10^{-11}$.

IV. GRAVITATIONAL LENSING BY SCHWARZSCHILD BLACK HOLE

In this section we provide a brief overview of the results related to the gravitational lensing of light in Schwarzschild black hole geometry. As we discuss later, the naked singularity geometry under investigation in this paper matches with the Schwarzschild geometry at the finite radial coordinate. Therefore for the light rays that stay in the Schwarzschild regime all the time, the

gravitational lensing is identical to that in Schwarzschild spacetime. In the next section we discuss change in the gravitational lensing properties due to the presence of the naked singularity and make a critical comparison with Schwarzschild results. The gravitational lensing by the Schwarzschild black hole was explored in detail in [13]. We discuss the relevant details and results here.

The Schwarzschild metric is given by

$$ds^2 = - \left(1 - \frac{2M}{r}\right) dt^2 + \left(1 - \frac{2M}{r}\right)^{-1} dr^2 + r^2 d\Omega^2 \quad (14)$$

For convenience we work in the dimensionless variable $x = \frac{r}{2M}$. The distance of closest approach is $x_0 = \frac{r_0}{2M}$.

A. Deflection angle and photon sphere

We now compute the deflection angle as a function of the distance of minimum approach. From (9), the Einstein deflection angle in the Schwarzschild spacetime in terms of the dimensionless variables is given by

$$\hat{\alpha}(x_0) = 2 \int_{x_0}^{\infty} \left(\frac{1}{1 - \frac{1}{x}}\right)^{1/2} \left[\left(\frac{x}{x_0}\right)^2 \left(\frac{1 - \frac{1}{x_0}}{1 - \frac{1}{x}}\right) - 1 \right]^{-1/2} \frac{dx}{x} - \pi \quad (15)$$

As stated earlier the Einstein deflection angle diverges when the distance of minimum approach is very close to the radius of the photon sphere as the light circles around the center multiple times. It turns out that there is a photon sphere in a Schwarzschild spacetime that can be obtained by solving (10) which is located at the radius $r = r_{ph} = 3M$ or in terms of dimensionless variable at $x = x_{ph} = 1.5$. Using (1) and (8) the distance of minimum approach x_0 can be translated into the image location θ as

$$\sin \theta = \frac{2M}{D_d} \frac{x_0}{\sqrt{1 - \frac{1}{x_0}}} \quad (16)$$

which allows us to write deflection angle $\hat{\alpha}$ as a function of image location (θ). We have plotted $\theta(x_0)$ in Fig2. It is a monotonically increasing function of x_0 .

We plot the Einstein deflection angle $\hat{\alpha}(\theta)$ in Fig3

We have made use here of the values of the different quantities we have chosen in a galactic central supermassive black hole scenario we discussed earlier. It is a monotonically decreasing function of θ . It diverges as we approach the photon sphere which corresponds to $\theta \approx 16.8$ microarcseconds.

B. Images

We now qualitatively describe the images formed due to the deflection of the light by Schwarzschild black hole in the galactic central supermassive object scenario. The images' locations can be obtained by solving the lens equation for the chosen source location. The image is said to be relativistic if the deflection of the light ray is larger than $3\frac{\pi}{2}$ as per the convention used in [13].

In the weak field limit when the impact parameter is large and the deflection angle is small a pair of nonrelativistic images are formed. They have opposite parities. For small enough impact parameter, we get relativistic images with large deflection. Theoretically there are infinitely many images formed on both sides of the optic axis i.e. with both positive and negative values of θ . The relativistic images are bunched together around $\theta \approx 16.8$ microarcseconds. This is an extremely important point that no images are formed between the the optic axis and $\theta \approx 16.8$ microarcseconds. As we discuss later the situation can be significantly different in the case of the naked singularity. More details on the location of the images and the magnification can be found in [13].

C. Einstein rings

As the Einstein deflection angle is a monotonically decreasing function as seen from Fig3, there is no radial critical curve present in the geometry. Location of the Einstein rings can be obtained by solving the lens equation with $\beta = 0$. The Einstein rings are said to be relativistic if the deflection angle larger than 2π as per the convention used in [13].

With our choice of parameters for galactic supermassive object scenario we get an equation $\tan \theta = \tan(\hat{\alpha} - \theta)$, which admits a solution $\hat{\alpha} = 2n\pi + 2\theta$. There is a nonrelativistic Einstein ring which can be obtained by solving this equation for θ with $n = 0$. It is located at $\theta = 1.15$ arcsecond. There are infinitely many Einstein rings that can be obtained by solving the above equation with different values of n . All the relativistic Einstein rings are located close to $\theta \approx 16.8$ microarcseconds. As in the case of images there are no Einstein rings located between the optic axis and $\theta = 16.8$ microarcseconds. In case of the naked singularity geometry that we are about to discuss, the situation is significantly different.

V. GRAVITATIONAL LENSING BY JMN NAKED SINGULARITY

In this section we study the gravitational lensing by a spacetime containing naked singularity. We imagine a hypothetical situation where the galactic supermassive object is modeled by a naked singularity solution described by a specific metric. We study the images and the Einstein rings in the same situation and make a comparison. The spacetime geometry (to be referred to as JMN solution henceforth in this paper) we will be dealing with is a naked singularity solution obtained in [16] as the end

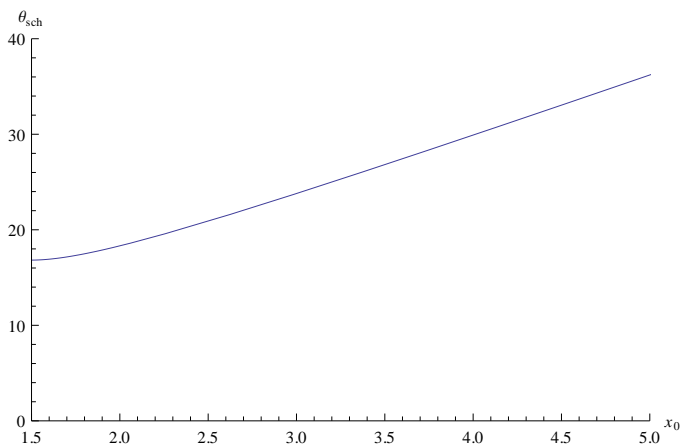


FIG. 2: θ vs x_0 in Schwarzschild spacetime. The image location θ (in microarcseconds) is plotted as a function of closest approach x_0 (dimensionless) in Schwarzschild spacetime for a galactic supermassive black hole scenario. It is a monotonically increasing function.

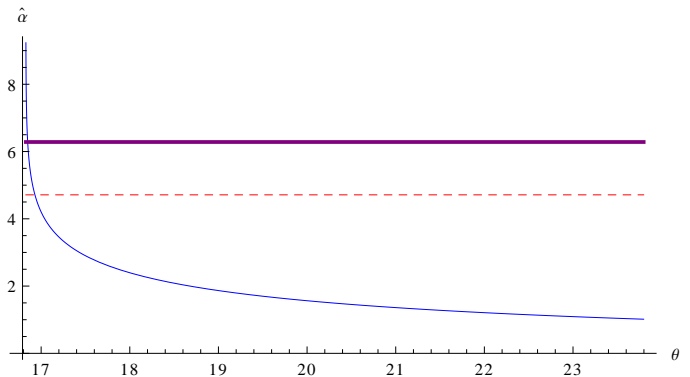


FIG. 3: $\hat{\alpha}$ vs θ : Einstein deflection angle $\hat{\alpha}$ (in radian) is plotted as a function of the image location θ (in microarcseconds) in Schwarzschild spacetime for a Galactic supermassive black hole scenario. $\hat{\alpha}(\theta)$ is monotonically decreasing. It diverges around $\theta \approx 16.8$ microarcseconds which corresponds to the photon sphere. The horizontal lines correspond to $3\pi/2$ and 2π for dashed (red) and thick (purple) lines respectively which mark the onset of the relativistic deflection of light. Relativistic images and Einstein rings can be seen between the photon sphere and the intersection points of horizontal lines with $\hat{\alpha}$ curve.

state of dynamical collapse from regular initial conditions for a fluid with zero radial pressure but non-vanishing tangential pressure. The solution has a naked singularity at the center and matches to a Schwarzschild spacetime across the boundary $r = R_b$. Basic features of accretion disks in such a model was studied by the same authors and differences with black hole case were pointed out. In the same spirit, gravitational lensing in this background would also be an interesting observational probe of the toy model.

A. JMN naked singularity geometry

The spacetime is divided into two parts. (a) The interior region which is described by the following metric:

$$ds_e^2 = -(1 - M_0) \left(\frac{r}{R_b} \right)^{\frac{M_0}{1-M_0}} dt^2 + \frac{dr^2}{1 - M_0} + r^2 d\Omega^2. \quad (17)$$

It can be easily shown that the curvature blows up at the center and thus it corresponds to a strong curvature time-like singularity. (b) The exterior region is described by a Schwarzschild solution

$$ds^2 = - \left(1 - \frac{M_0 R_b}{R} \right) dt^2 + \frac{dr^2}{(1 - M_0 R_b / r)} + r^2 d\Omega^2. \quad (18)$$

There is no event horizon in this geometry and thus the singularity at the center is exposed to the asymptotic observer at infinity. Therefore it is a naked singularity.

It can be easily verified that the two metrics are connected across the boundary $R = R_b$ via C^2 matching.

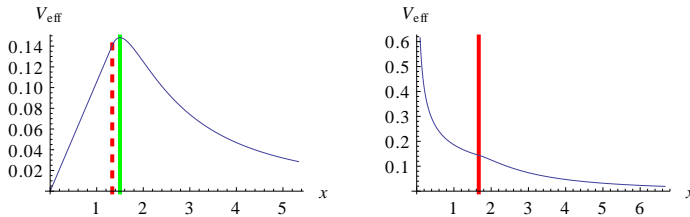


FIG. 4: V_{eff} vs x : Plotted here is the effective potential V_{eff} (dimensionless) for the radial motion for the light rays as a function of x (dimensionless). The plot on the left corresponds to the parameter values $M_0 \geq 2/3$. The thick (green) vertical line corresponds to the photon sphere, whereas the dashed (red) line corresponds to the boundary between the interior naked singularity region and exterior Schwarzschild geometry. The effective potential monotonically goes to zero in the interior region. The plot on right corresponds to the parameter values $M_0 < 2/3$, where the photon sphere is absent. The vertical red line is the boundary. The effective potential blows up as we approach the singularity.

There are two parameters in the solution, M_0 which is a dimensionless parameter and, R_b which is the boundary radius at which the interior naked singularity metric is matched to the exterior Schwarzschild metric. We must have $0 < M_0 < 1$. The Schwarzschild mass is related to these two parameters by a relation $M = \frac{M_0 R_b}{2}$. We fix the Schwarzschild mass to be same as we had chosen in the previous section for the sake of comparison. Thus for fixed M the only free parameter happens be M_0 . The boundary between the two region is related to M_0 as $R_b = \frac{2M}{M_0}$.

As in the Schwarzschild black hole case we introduce the dimensionless variable $x = \frac{r}{2M}$, where all the distances are expressed in units of the Schwarzschild radius. Thus the impact parameter is $x_0 = \frac{r_0}{2M}$ and the boundary radius becomes simply the inverse of the parameter M_0 i.e. $x_b = \frac{R_b}{2M} = \frac{1}{M_0}$. Thus larger the parameter M_0 , smaller is the radius of the boundary for a given mass M and we have a more compact object.

B. Deflection angle

We now compute the deflection angle. The first question one would like to ask for lensing in strong field regime is whether photon sphere is present in the spacetime, since the bending angle $\hat{\alpha}$ would diverge as the distance of closest approach tends to x_{ph} where $x = x_{ph}$ is the location of the photon sphere.

In order to investigate the existence of the photon

sphere or otherwise and its location we look for the maximum of the effective potential $V_{\text{eff}} = \frac{g(r)}{r^2}$ or in other words we solve the equation (10).

When $M_0 \geq \frac{2}{3}$ the boundary between the interior and exterior Schwarzschild region is at $x_b = \frac{1}{M_0} \leq \frac{3}{2}$. So the boundary is below the photon sphere in the exterior Schwarzschild region $x \leq x_{ph}$. The effective potential for the radial motion of the light ray is plotted in Fig4(left part). The effective potential goes on decreasing below the photon sphere and asymptotically goes to zero. It is clear from the behavior of the effective potential that the light ray which enters the photon sphere never turns back and it eventually hits the naked singularity. Thus it is captured. Photons can turn back from the region exterior to the photon sphere and deflection angle goes on increasing indefinitely as we approach approach it. This implies that the lensing will be exactly identical to Schwarzschild case which we discussed in the previous section as it is not possible for photons coming from and going back to a large distance probe the metric interior to photon sphere. Thus the gravitational lensing cannot unravel the possible existence of the naked singularity at the center for $M_0 \geq \frac{2}{3}$.

When $M_0 < \frac{2}{3}$ the boundary is located at $x_b = \frac{1}{M_0} > \frac{3}{2}$. Thus there is no Schwarzschild photon sphere in the exterior region, since the boundary is outside the location of the Schwarzschild photon sphere $x_b > x_{ph}$. The effective potential for the radial motion for the light rays is plotted in Fig4(right part). The effective potential is monotonically decreasing function in the interior region. Since it does not admit any extremum, no photon sphere is present in the interior region as well. The effective potential in fact blows up at the singularity which implies that no light ray can reach it.

From now on wards we focus on the case $M_0 < \frac{2}{3}$. If the distance of minimum approach is larger than $x_0 \geq x_b = \frac{1}{M_0}$, then the light ray travels in the exterior Schwarzschild geometry and the images and Einstein rings formed due to the lensing are identical to those discussed in the previous section. Thus we focus on the case where the distance of minimum approach is less than the boundary radius $x_0 < x_b = \frac{1}{M_0}$. So that the light rays travel partly in the external Schwarzschild metric and partly in the interior metric and it can actually probe the interior, containing naked singularity. We would like to understand the formation of images and the Einstein rings due to the light rays passing through the interior region.

The Einstein deflection as a function of distance of closest approach when $x_0 < \frac{1}{M_0}$ is given by

$$\hat{\alpha}(x_0) = 2 \int_{x_0}^{\frac{1}{M_0}} \left(\frac{1}{1-M_0} \right)^{1/2} \left[\left(\frac{x}{x_0} \right)^2 \left(\frac{x_0}{x} \right)^\gamma - 1 \right]^{-1/2} \frac{dx}{x} + 2 \int_{\frac{1}{M_0}}^{\infty} \left(\frac{1}{1-\frac{1}{x}} \right)^{1/2} \left[\left(\frac{x}{x_0} \right)^2 \frac{(1-M_0)(x_0 M_0)^\gamma}{1-\frac{1}{x}} - 1 \right]^{-1/2} \frac{dx}{x} - \pi \quad (19)$$

where $\gamma = \frac{M_0}{1-M_0}$. The first term corresponds to the contribution to the deflection angle from the interior region and the second term corresponds to the contribution from the exterior Schwarzschild region.

Using the relationship between θ and x_0 , i.e.

$$\sin \theta = \frac{2M}{D_d} \frac{x_0}{\sqrt{(1-M_0)(x_0 M_0)^\gamma}} \quad (20)$$

we can express deflection angle as a function of image location $\hat{\alpha}(\theta)$. We have plotted $\theta(x_0)$ for the geometry in Fig5 and $\hat{\alpha}(\theta)$ in Fig6.

Presence of the photon sphere guarantees the relativistic deflection of light, though, as we pointed out earlier, it prevents probes to the interior density structure. But we are investigating the parameter regime $M_0 < \frac{2}{3}$ where the photon sphere is absent in the geometry. So the relativistic deflection may or may not occur. Firstly we would like to find out the parameter range M_0 where we expect relativistic deflection of light to happen.

Looking at the Fig3 and Fig 6, Einstein deflection angle is monotonically increasing with decreasing x_0 for both Schwarzschild and JMN. In Schwarzschild geometry the deflection angle reaches $\frac{3\pi}{2}$ at $x_0 \sim 1.605$ i.e. if $M_0 > 0.62$. So any x_b less than that (and hence $M_0 > 0.62$) will definitely give relativistic deflection. This is sufficient but not necessary condition. More detailed calculation shows that the maximum value of the deflection angle is larger than 2π for $M_0 > 0.475$. Thus relativistic images

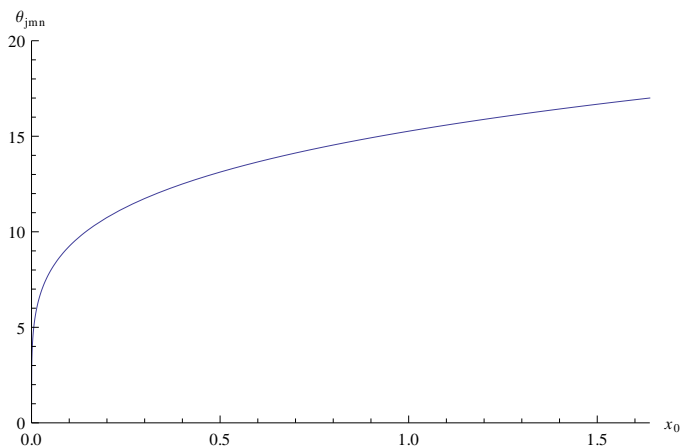


FIG. 5: θ vs x_0 in JMN: The image location θ (in microarcseconds) is plotted as a function of closest approach x_0 (dimensionless) in JMN spacetime for a galactic central supermassive object scenario in an interior region. It is a monotonically increasing function.

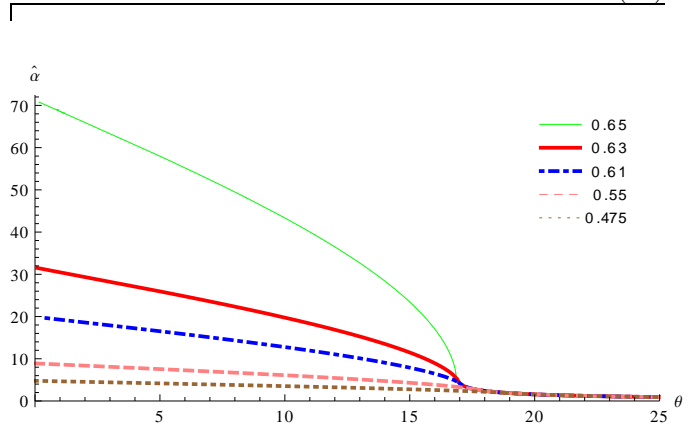


FIG. 6: $\hat{\alpha}$ vs θ for different M_0 : Einstein deflection angle $\hat{\alpha}$ (in radian) in JMN spacetime is plotted against the image location θ (in microarcseconds). The value of M_0 for the curves are shown in the legends. $\hat{\alpha}$ is a monotonically decreasing function. As we increase M_0 the maximum deflection angle goes on increasing. The deflection angle will be larger than 2π and thus relativistic images can form for $M_0 > 0.475$. The curves for different values of M_0 cross because ultimately all the curves have to match to the deflection angle curve for Schwarzschild spacetime beyond the boundary and since boundary $x_b = \frac{1}{M_0}$ is at the smaller radius for larger M_0 .

and Einstein rings can form beyond this parameter value. Note that this is independent any value of Schwarzschild mass.

C. Images

We now describe the properties of the images formed due to the gravitational lensing of the light passing through the interior region. The relativistic images are possible only beyond the parameter value $M_0 > 0.475$. These images probe the interior geometry and can unravel existence of the naked singularity.

We calculate the location of the images and their magnification for galactic supermassive object scenario with a given source location that is in the near-aligned configuration. We solve the lens equation for fixed $\beta = 0.075$ and for given $M_0 > 0.475$. For different values of M_0 we get different number of images on the same side as well as on the opposite side of the optic axis. The number of image goes on increasing as we increase M_0 .

In Table I,II we make a list of image locations and magnifications for a specific value of $M_0 = 0.63$. There are four images on the same side as well as on opposite side of the optic axis. Images are well separated

TABLE I: Images and magnification (same side): In this table we list the location of the relativistic images and magnifications on the same side as source for the galactic central supermassive object scenario for $M_0 = 0.63$ and $\beta = 0.075$ radian. θ is in microarcseconds. The images are well separated and have comparable magnifications

Image	θ	μ_t	μ_r	μ
I	16.74	1.9×10^{-9}	1.8×10^{-12}	1.9×10^{-21}
II	14.56	0.9×10^{-9}	4.7×10^{-12}	4.4×10^{-21}
III	10.75	0.7×10^{-9}	6.8×10^{-12}	5.0×10^{-21}
IV	5.82	0.4×10^{-9}	8.0×10^{-12}	3.2×10^{-21}

TABLE II: Images and magnification (opposite side): In this table we list the location of the relativistic images and magnifications on the opposite side as source for the galactic central supermassive object scenario for $M_0 = 0.63$ and $\beta = 0.075$ radian. θ is in microarcseconds. The images are well separated and have comparable magnifications.

Image	θ	μ_t	μ_r	μ
I	16.68	-1.1×10^{-9}	1.9×10^{-12}	-2.1×10^{-21}
II	14.41	-0.9×10^{-9}	4.8×10^{-12}	-4.4×10^{-21}
III	10.54	-0.7×10^{-9}	6.9×10^{-12}	-4.7×10^{-21}
IV	5.58	-0.4×10^{-9}	8.1×10^{-12}	-3.0×10^{-21}

from one another with angular separation of around 2-5 microarcsecond. The magnification of all the images is of the same order of magnitude. The radial parity of the image is always positive. The tangential parity and thus the total parity is positive for the images on the same side of the optic axis while it is negative for the images on the opposite side. Also it is worthwhile to mention here that the position of relativistic images does not change much with changes in source position which can also be inferred from the fact that the radial magnification of the images (which is $\frac{d\theta}{d\beta}$) is of the order of 10^{-12} as shown in tables I and II.

D. Einstein rings

Since the deflection angle is a monotonically decreasing function of the image location the radial critical curves

VI. COMPARISON WITH SCHWARZSCHILD BLACK HOLE

In this section we make a critical comparison of the results obtained for gravitational lensing in Schwarzschild black hole and naked singularity geometry described by JMN solution with the same mass in a galactic central supermassive object scenario.

In the Schwarzschild black hole case the photon sphere is present. Apart from the outer nonrelativistic images

would be absent. The caustic happens to be a point $\beta = 0$, since we are dealing with spherically symmetric

TABLE III: Einstein rings: In this table we list the location of the relativistic Einstein rings for $M_0 = 0.63$ for the galactic central supermassive scenario and the corresponding values of the deflection angle, θ is in microarcseconds and $\hat{\alpha}$ is in radian. The Einstein rings are well separated.

No.	θ_E	$\hat{\alpha}$
I	16.715	$2\pi + 0.00068$
II	14.485	$4\pi + 0.00042$
III	10.469	$6\pi + 0.00076$
IV	5.700	$8\pi + 0.00173$

spacetimes. In order to compute the critical curves i.e. the location of the Einstein rings we solve the lens equation with $\beta = 0$. As discussed in the Schwarzschild case for the galactic supermassive object scenario, we have to solve the equation $\tan \theta = \tan(\hat{\alpha} - \theta)$, which holds good when $\hat{\alpha} = 2n\pi + 2\theta$. Knowing $\hat{\alpha}$ we can solve the previous equation to get the angular locations of the Einstein rings. For a given value of M_0 , the number of solutions to this equation would be either $\lceil \frac{\hat{\alpha}_{max}}{2\pi} \rceil$ or $\lfloor \frac{\hat{\alpha}_{max}}{2\pi} \rfloor - 1$ which will be the number of the relativistic Einstein rings. The number of the relativistic Einstein rings goes on increasing as we increase M_0 . As in the Schwarzschild case there will be a nonrelativistic Einstein ring located at 1.15 arcsecond which corresponds to the solution of the equation with $n = 0$.

For $M_0 = 0.63$ we have four relativistic Einstein rings. The location of the relativistic Einstein rings and the corresponding Einstein deflection angles is given in Table III. The rings are well separated from one another with separation of the order of 2-5 microarcseconds.

In Fig 7, 8, 9, we show the variation of the tangential, radial and total magnification with θ near the relativistic Einstein rings. As expected tangential and consequently total magnification diverges at the Einstein rings and falls rapidly as we move away from it.

and Einstein ring, infinite number of relativistic images and Einstein rings are formed. But they are clumped together around $\theta \approx 16.8$ microarcseconds. No images or rings are formed between the optic axis and $\theta \approx 16.8$ microarcseconds which happens to be the forbidden region. The separation between the first and rest of the images clumped together is of the order of 0.1 microarcseconds and the ratio of magnifications is of the order of 500 [13, 19, 20].

In JMN geometry when $M_0 \geq \frac{2}{3}$ Schwarzschild photon

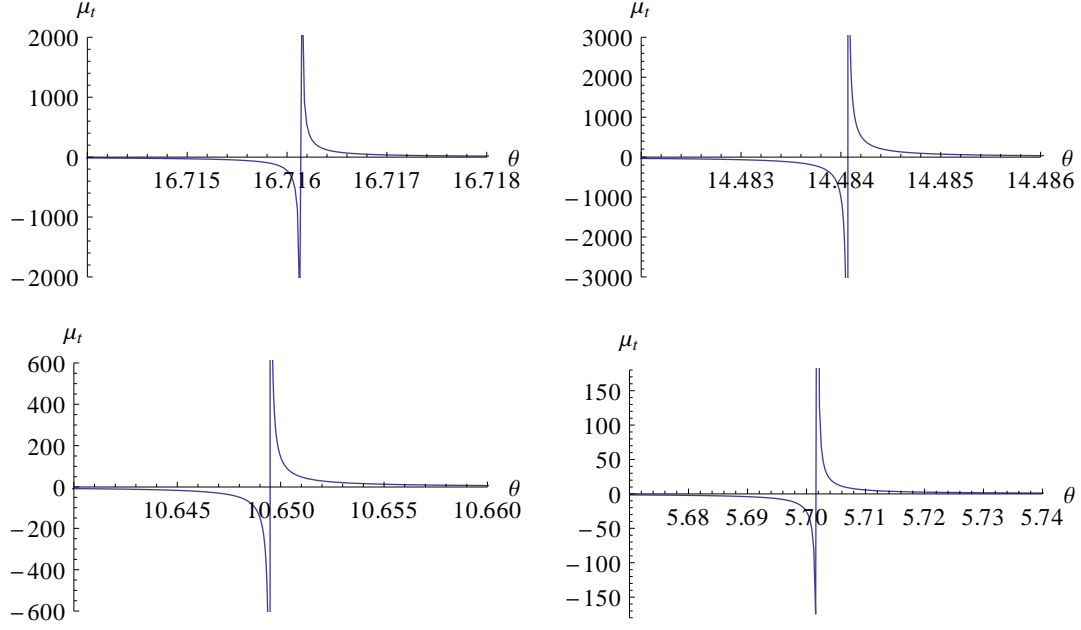


FIG. 7: μ_t vs θ for JMN spacetime: Plotted here is the tangential magnification near the Relativistic Einstein Rings for $M_0 = 0.63$. θ is in microarcseconds and y-axis scale has been multiplied by 10^9 for clarity. Tangential magnification blows up at the location of the Einstein ring and decreases as we go away from it.

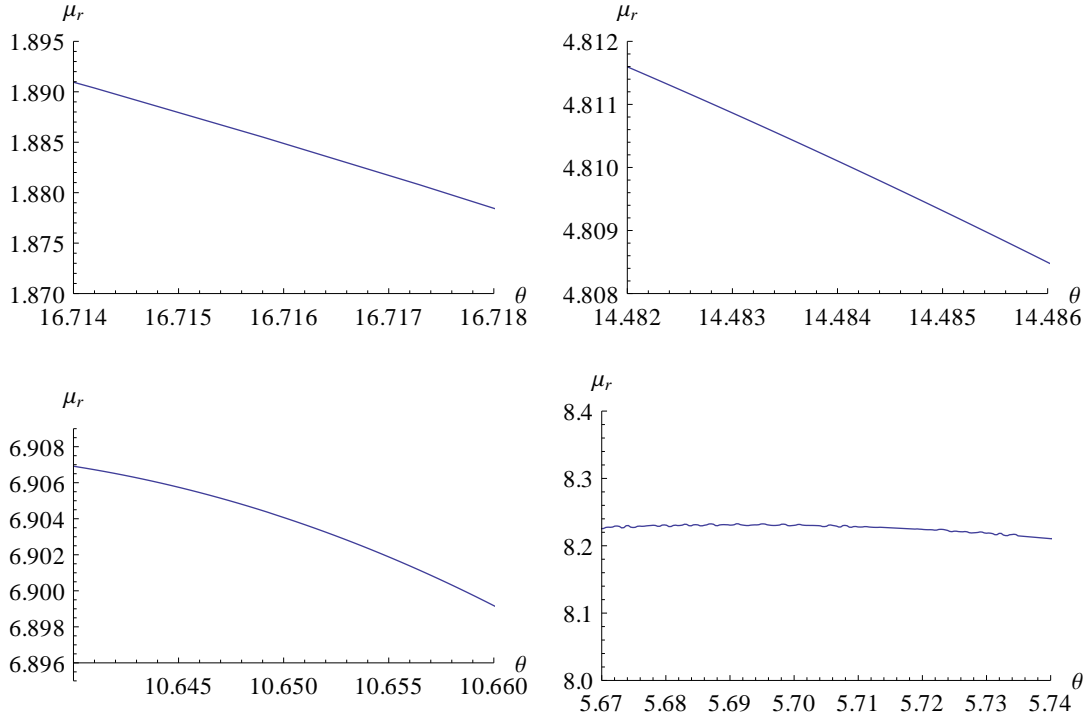


FIG. 8: μ_r vs θ for JMN spacetime: Plotted here is the radial magnification near the Relativistic Einstein Rings for $M_0 = 0.63$. θ is in microarcseconds and y-axis scale has been multiplied by 10^{12} for clarity.

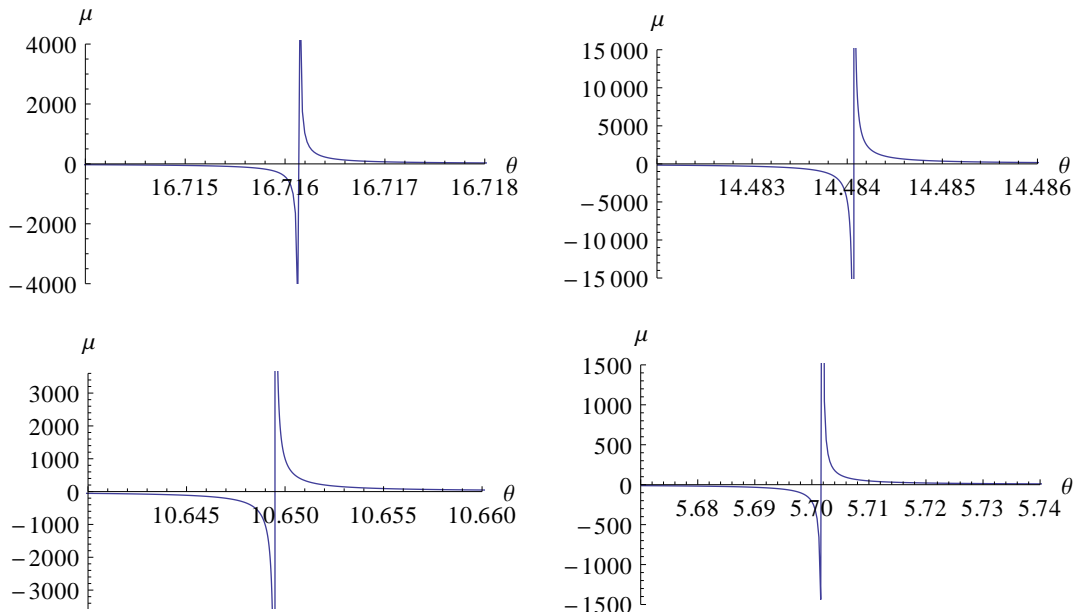


FIG. 9: μ vs θ for JMN spacetime: Plotted here is the total magnification near the Relativistic Einstein Rings for $M_0 = 0.63$. θ is in microarcseconds and y-axis scale has been multiplied by 10^{21} for clarity. Total magnification blows us at the location of the Einstein ring and decreases as we go away from it.

sphere is present and the gravitational lensing is identical to that of Schwarzschild black hole. If $M_0 \leq 0.475$ no relativistic images are formed.

The interesting regime in parameter space is $0.475 < M_0 < \frac{2}{3}$. A number of relativistic images and Einstein rings are formed depending on how large is M_0 . Unlike Schwarzschild black hole case the images are not clumped together. They are well separated from one another. Images and Einstein rings can appear in the region between optic axis and $\theta \approx 16.8$ microarcseconds which is a forbidden region for Schwarzschild black hole. The images have comparable magnifications.

Thus there are qualitative differences in the images formed in Schwarzschild black hole geometry and JMN spacetime when $M_0 < \frac{2}{3}$. These features can in principle lead to the observational distinction between the two spacetimes.

VII. COMPARISON WITH JNW NAKED SINGULARITY

In the previous section we compared the gravitational lensing in Schwarzschild black hole geometry with that of JMN naked singularity. In this section we make a comparison between JMN naked singularity and JNW naked singularity which has been studied in the past from the perspective of strong gravitational lensing [4], [5]. It is a solution of Einstein equations with a minimally coupled massless canonical scalar field with two parameters, mass M and scalar charge q . For low scalar charge $\frac{q}{M} \leq \sqrt{3}$ this solution has a photon sphere. In this case the quali-

tative features of lensing are very similar to Schwarzschild case.

However, for large scalar charge $\frac{q}{M} > \sqrt{3}$ photon sphere is absent in JNW spacetime. It was stated in [5] that the relativistic deflection and images are absent completely in the absence of the photon sphere. However, a careful investigation in this range of parameters shows that in an extremely small range of parameter $\sqrt{3} < \frac{q}{M} \leq 1.746$, relativistic lensing and images are formed even in the absence of the photon sphere. Relativistic images are absent when $\frac{q}{M} > 1.746$. But interestingly as mentioned in [5] the radial caustic is always present in the absence of the photon sphere. This is a consequence of the fact that as we decrease the impact parameter the deflection angle initially increases, it attains a maximum and goes on decreasing. Eventually it settles down to a constant negative value $-\pi$ in the limit where impact parameter approaches zero.

In the JMN spacetime, in the absence of the photon sphere we get relativistic images in a rather wide range of parameter values $0.475 < M_0 < \frac{2}{3}$ as compared to JNW case. Relativistic images are absent for $M_0 < 0.475$. However, radial caustic is always absent in JMN geometry. Thus the radial caustic will allow us to distinguish between JNW and JMN naked singularities in the absence of the photon sphere.

We note that the massless scalar fields are not observed in nature. Also it is not clear whether or not JNW solution is an endstate of the gravitational collapse. Thus it would be worthwhile to study other realistic solutions containing naked singularities which might be an endstate of the gravitational collapse to see whether they ex-

hibit lensing signature which is quite different from JNW spacetime. The JMN spacetime that we study in this paper is a toy model with zero radial pressure, but it has the merit of being obtainable as a possible endstate of the gravitational collapse. As we have shown, the gravitational lensing in JMN spacetime can be significantly different from that in JNW geometry in the appropriate parameter range. In future we intend to study the lensing in the more realistic spacetime with nonvanishing radial pressure and also which is the endstate of gravitational collapse.

VIII. OBSERVABILITY OF RELATIVISTIC IMAGES IN A REALISTIC SCENARIO

So far we studied the gravitational lensing in an idealized scenario and showed that JMN naked singularity can in principle be distinguished from Schwarzschild black hole and JNW naked singularity by the observation of the relativistic images and Einstein rings. In this section we try to gauge the possibility of observation of the relativistic images in a realistic scenario with the current state of art instruments and techniques.

The distance of relativistic images from the optic axis is of the order of $\frac{M}{D} \approx 10$ microarcseconds and their magnification is of the order of $\mu \approx 10^{-21}$. The angular distance from the optic axis is extremely small. Larger the mass and smaller the distance of the observer to the lens, larger will be the angular separation from the optic axis. It might be possible to achieve microarcseconds resolution with Very Long Base Interferometry (VLBI) [23]. However since the magnification is extremely small the observation of these images seems difficult.

As we discussed earlier, magnification of the Einstein rings with point sources is infinite. However in reality we deal with the sources of finite extent. We now estimate the expected values of the magnification for Einstein rings with source which is taken to be a star like the sun with radius $R \approx 7 \cdot 10^8 m$. As discussed earlier in the galactic central supermassive object scenario, the distance of the sun as well as the sun-like star which acts as a source is $D \approx 8.5 kpc$. Orbital velocity of such a star will be comparable to that of sun $v \sim 220$ km/sec. The angle subtended by the star at the observer in a near aligned lensing situation would be $\Delta\beta = \frac{2R}{D} \approx 1$ microarcseconds. The angular radius of the outer non-relativistic Einstein ring as in the case of Schwarzschild spacetime would be around $\theta_E \approx \sqrt{\frac{M}{D}} \approx 1 arcsec$, whereas radius of the Einstein rings formed due to the relativistic deflection would be $\theta_E \approx \frac{M}{D} \approx 10$ microarcseconds. In a realistic scenario a star with the finite extent is not stationary but moves around with the orbital velocity and therefore the Einstein rings would appear only when the star crosses the caustic $\beta = 0$ and would last for a time $\Delta T = \frac{R}{v} \approx 3200 sec \approx 50 min$, whereas the time delay between the arrival of photons along the different trajec-

tories leading to different rings would be of the order of $\tau \approx \frac{GM}{c^3} \approx 10 sec$. Thus all the rings would appear and disappear almost simultaneously. The tangential magnification for a finite source is not infinite but takes an approximate value $\mu_t \approx \frac{\theta_E}{\Delta\beta}$. This expression can be derived easily for the external image by computing an averaged tangential magnification for the finite size source. The average radial magnification is of the same order as the radial magnification at Einstein ring as it varies very slowly with image position. Thus the tangential magnification of the outer non-relativistic Einstein ring would be $\mu_t \approx 10^6$, whereas that of inner relativistic Einstein rings would be $\mu_t \approx 10$. The radial magnification of non-relativistic ring is of order 1 while that of relativistic rings is 10^{-12} . Then the total magnification of the outer rings is seventeen orders of magnitude larger than that of the inner rings. So it is doubtful that inner rings will be visible in the presence of the outer ring which is much more brighter with the current state of art instruments which may not have sensitivity over such a large range of magnification.

It seems that it may not be possible to unravel the true nature of the galactic central supermassive object at present as the inner images which carry the information about the possible existence of the naked singularity are swamped by the bright outer image which provides the information only about the Schwarzschild mass. We note that this is always going to be a generic feature associated with relativistic images and would be independent of the specific naked singular metric under consideration.

However keeping this point in mind dedicated instruments and techniques could be developed in the future which might be able to unravel the possible existence of a naked singularity instead of black hole.

IX. GRAVITATIONAL LENSING DUE TO A BINARY SYSTEM AS A PROBE OF COSMIC CENSORSHIP

In this section we propose a scenario where one might be able to test the cosmic censorship with the current state of instruments and technology available to us. The assumption of the spherical symmetry made in this paper for the sake of simplicity is unrealistic. In the absence of spherical symmetry the caustic will be fairly complicated and not just a point. For instance one could imagine a situation where the evolution of the massive binary star system has eventually led to the configuration consisting of the naked singularity and an ordinary star orbiting around each other. If one of the star is massive as compared to the other it will die much earlier. As an example $50 M_\odot$ star would die in 0.5 million years and could possibly turn into a naked singularity instead of a black hole. The main caustic in this scenario could be diamond shaped with cusps. A given source might cross caustics multiple times giving rise to the appearance and disappearance of the Einstein rings or large magnified images

multiple times. Time difference between the disappearance and reappearance of the consecutive Einstein rings will be influenced by the presence of the naked singularity in the binary system. Thus it could be used to infer the presence of naked singularity, as against a black hole. Such a situation is however extremely difficult to model. It is beyond the scope of this paper and might be dealt with later.

X. CONCLUSION AND DISCUSSION

In this paper we studied the strong gravitational lensing from the perspective of cosmic censorship and explored the possibility of distinguishing black holes from naked singularities. We modeled the galactic central supermassive dark object initially by a black hole and then by naked singularity. We studied the gravitational lensing of the source in a near aligned configuration at a distance from a galactic center approximately comparable to distance of the sun from the center.

The Schwarzschild black hole has a photon sphere. Thus apart from a pair of nonrelativistic images and a nonrelativistic Einstein ring, infinitely many relativistic images and Einstein rings clumped together. No images and Einstein rings lie in the region between the optic axis and $\theta = 16.8$ microarcseconds. Also all the images that are clumped together are highly demagnified as compared to the first relativistic image with a small separation between them of the order of 0.1 microarcseconds.

We then model the galactic center object as JMN solution which was recently shown to occur as an end state of the gravitational collapse of a fluid with zero radial pressure but non-vanishing tangential pressure. This solution has two parameters, namely mass and another parameter M_0 . The spacetime is divided into two parts. Exterior metric is Schwarzschild spacetime with same mass as that of the Schwarzschild black hole considered earlier. Interior metric contains a central naked singularity with the boundary located at the radius $R_b = \frac{2M}{M_0}$. The two metrics are connected across the boundary by C^2 matching.

In the parameter range $M_0 \geq \frac{2}{3}$ the Schwarzschild photon sphere is present in the geometry and the gravitational lensing signature of JMN spacetime is identical to that of the Schwarzschild black hole.

When $M_0 \leq 0.475$, the photon sphere is absent. But no relativistic bending of light and thus no relativistic images possible. This behavior is different from the Schwarzschild black hole.

The interesting parameter range is when $0.475 < M_0 <$

$\frac{2}{3}$. The photon sphere is absent. But the relativistic images and Einstein rings can form and their number increases with increasing value of the parameter M_0 . The images and rings are well separated from one another and happen to lie in the forbidden region for Schwarzschild black hole, within a distance from the optic axis of $\theta = 16.8$ microarcseconds. Their magnification is also comparable. Thus the strong gravitational lensing signature is qualitatively different from Schwarzschild black hole.

The gravitational lensing in the absence of the photon sphere is qualitatively different in JMN and JNW spacetimes. In both the geometries relativistic images are present in an appropriate parameter range. However, there are no radial caustics in the JMN geometry, while radial caustic is always present in the JNW spacetime in the absence of the photon sphere.

However, there are practical difficulties as far as observation of relativistic images and rings are concerned with the telescopes and techniques currently being used. We require microarcseconds resolution which can be achieved with VLBI. However magnification of the images which is of the order of $\mu = 10^{-22}$ is too small. Relativistic Einstein rings formed due to the lensing of the star with the size comparable to sun, will be 10^{17} times weaker as compared to the nonrelativistic Schwarzschild Einstein ring and thus will not be seen since the current instruments do not have dynamical range over seventeen orders of magnitude of brightness.

Keeping this in mind, new techniques and instruments must be developed in the future which will be able to observe the Einstein rings and can unravel the nature of the galactic central supermassive object.

We also suggest that the appearance and disappearance of the outer Einstein ring as the source crosses diamond shaped caustic more than once can possibly shed light on the possible existence of the naked singularity in the binary system of a naked singularity and a massive star. We wish to explore this situation in the future.

In this paper we studied a naked singularity geometry arising out of a toy calculation of dynamical collapse of a matter with only the tangential pressure. It would be interesting to study more realistic cases e.g. with the inclusion of the radial pressure.

Acknowledgments

We thank K.S.Virbhadra and the anonymous referee for valuable comments and suggestions.

-
- [1] R. Penrose, Nuovo Cimento Rivista Serie **1**, 252 (1969).
 [2] P. S. Joshi, *Gravitational Collapse and Spacetime Singularities* (Cambridge University Press, 2007).
 [3] P. S. Joshi and D. Malafarina, International Journal of

- Modern Physics D **20**, 2641 (2011), 1201.3660.
 [4] K. Virbhadra, D. Narasimha, and S. Chitre, *Astron.Astrophys.* **337**, 1 (1998), astro-ph/9801174.
 [5] K. S. Virbhadra and G. F. Ellis, *Phys. Rev. D* **65**, 103004

- (2002).
- [6] M. Werner and A. Petters, *Phys.Rev.* **D76**, 064024 (2007), 0706.0132.
- [7] G. N. Gyulchev and S. S. Yazadjiev, *Phys.Rev.* **D78**, 083004 (2008), 0806.3289.
- [8] C. Bambi and N. Yoshida, *Class.Quant.Grav.* **27**, 205006 (2010), 1004.3149.
- [9] C. Bambi and K. Freese, *Phys.Rev.* **D79**, 043002 (2009), 0812.1328.
- [10] K. Hioki and K.-i. Maeda, *Phys.Rev.* **D80**, 024042 (2009), 0904.3575.
- [11] C. Darwin, *Royal Society of London Proceedings Series A* **249**, 180 (1959).
- [12] C. Darwin, *Royal Society of London Proceedings Series A* **263**, 39 (1961).
- [13] K. S. Virbhadra and G. F. R. Ellis, *Phys. Rev. D* **62**, 084003 (2000), arXiv:astro-ph/9904193.
- [14] M. P. Dabrowski and F. E. Schunck, *Astrophys. J.* **535**, 316 (2000), arXiv:astro-ph/9807039.
- [15] N. Bilić, H. Nikolić, and R. D. Viollier, *Astrophys. J.* **537**, 909 (2000), arXiv:astro-ph/9912381.
- [16] P. S. Joshi, D. Malafarina, and R. Narayan, *Class.Quant.Grav.* **28**, 235018 (2011), 1106.5438.
- [17] S. Frittelli, T. P. Kling, and E. T. Newman, *Phys. Rev. D* **61**, 064021 (2000), arXiv:gr-qc/0001037.
- [18] V. Perlick, *Phys. Rev. D* **69**, 064017 (2004), arXiv:gr-qc/0307072.
- [19] V. Bozza, *Phys. Rev. D* **66**, 103001 (2002), arXiv:gr-qc/0208075.
- [20] V. Bozza, S. Capozziello, G. Iovane, and G. Scarpetta, *General Relativity and Gravitation* **33**, 1535 (2001), arXiv:gr-qc/0102068.
- [21] E. F. Eiroa and C. M. Sendra, *Classical and Quantum Gravity* **28**, 085008 (2011), 1011.2455.
- [22] A. Bhadra, *Phys. Rev. D* **67**, 103009 (2003), arXiv:gr-qc/0306016.
- [23] J. S. Ulvestad, *New Astron.Rev.* **43**, 531 (1999), astro-ph/9901374.